Readsorption and Adsorption-Assisted Desorption of CO_2 on Basic Solids

Mingting Xu and Enrique Iglesia*

Department of Chemical Engineering, University of California, Berkeley, California 94720

Received: July 7, 1997; In Final Form: October 10, 1997

The desorption of $^{13}CO_2$ from the surface of basic oxides based on modified MgO was examined at conditions of chemical equilibrium using a $^{13}CO_2/^{12}CO_2$ isotopic switch method. $^{13}CO_2$ desorption rates increase with increasing concentration of $^{12}CO_2$ in the gas phase and with increasing carrier gas flow rate, both during isotopic switch and transient temperature-programmed desorption of CO_2. These effects are caused by a decrease in the probability of $^{13}CO_2$ readsorption and not by faster desorption steps assisted by gas-phase $^{12}CO_2$. This isotopic switch method allows the determination of desorption rates and of the density of sites that can bind CO_2 reversibly at conditions typical of steady-state catalytic reactions. These measurements require, however, that we include in data analysis protocols any effects of readsorption processes.

Introduction

Several studies have shown that the rate of CO desorption from metal surfaces increases when CO is also present in the contacting gas phase.[1−6] Tamaru and co-workers[1−3] used a $C^{18}O/C^{16}O$ isotopic jump method to detect the rates of $C^{18}O$ desorption from Pd and Rh polycrystalline surfaces and found that the rate of desorption in the presence of gas-phase $C^{16}O$ is faster than in a vacuum. These authors reported that desorption rates of $C^{18}O$ were proportional to the pressure of $C^{16}O$ in the gas phase. This phenomenon was labeled "adsorption-assisted desorption". Goodman et al.[6] used temperature-programmed desorption to show that $C^{18}O$ desorption rates from Ni(100) surfaces were slower when desorption occurred in an ultrahigh-vacuum environment than when it occurred from a surface exposed to a high flux of $C^{16}O$ molecules. Desorption peaks shifted to lower temperatures in the presence of gas-phase CO. Other gas-phase molecules, such as H_2[7,8] and C_2H_2,[9] also increased CO desorption rates from metal surfaces. Some of these studies involved transient conditions leading to changes in surface coverage with changes in gas-phase atmosphere, time, and temperature. In such cases, enhanced desorption rates can reflect repulsive intermolecular interactions that lower desorption activation energies as coverage increases.

Zhdanov[10] proposed that the studies of Tamaru et al.[2,3] overestimated desorption rates and that the pressure dependence of the desorption rate reflects the dependence of desorption activation energy on surface coverage. He found that the observed desorption rates appear to depend on gas-phase pressure when desorption activation energies decrease with increasing surface coverage.[10] Simulations of desorption spectra by Lombardo and Bell[11] using Monte Carlo methods showed that desorption rates increase as desorption proceeds during transient experiments for adsorbed species with repulsive intermolecular interactions. The presence of gas-phase CO increases surface coverage and consequently lowers the desorption activation energy in such systems. By accounting for the coverage-dependent desorption activation energy, Weinberg et al.[12] found similar desorption rates under vacuum and in the presence of a CO background pressure on Ir(111) surfaces. Thus "adsorption-assisted desorption" effects can be ruled out at least for CO desorption on Ir(111) surfaces.

In our study, phenomena with a strong symptomatic resemblance to adsorption-assisted desorption are examined by measuring CO_2 desorption rates from 1.0 wt % K−MgO and 3.5 wt % K−$Cu_{0.5}Mg_5CeO_x$ porous solids at conditions of adsorption−desorption chemical equilibrium using a $^{13}CO_2/^{12}CO_2$ isotopic switch method. This technique was previously used in order to measure the number of available CO_2-bound sites on these samples at temperatures typical of catalytic reactions.[13,14] Isotopic switch methods have also been widely used to measure the surface density and pool of reactive intermediates during catalytic reactions.[15−20] Our study confirms the previously observed increase in $^{13}CO_2$ desorption rate with increasing concentration of gas-phase $^{12}CO_2$. These phenomena, however, are caused by the lower rate of $^{13}CO_2$ readsorption as the surface coverage of CO_2 increases and the number of surface vacant adsorption sites decrease with increasing CO_2 gas-phase concentrations.

Experimental Section

MgO and $Cu_{0.5}Mg_5CeO_x$ samples promoted by potassium were prepared by coprecipitation of aqueous metal nitrates with a solution of potassium hydroxide and potassium carbonate at 338 K and a constant pH of 9, as described in detail elsewhere.[13] $^{13}CO_2/^{12}CO_2$ isotopic switch experiments were carried out by dehydrating a catalyst sample (25−75 mg, 80−140 mesh) in flowing He (100 mL/min) at 723 K for 0.3 h. The Cu-containing sample was treated with a 5% H_2/He stream at 623 K for 0.5 h in order to reduce CuO to Cu. These pretreatment procedures lead to active alcohol synthesis catalysts.[13]

These samples were then exposed to a stream containing 0.1% $^{13}CO_2$/0.1% Ar/He (100 cm^3/min; Cambridge Isotopes Inc.) at 573 K. After $^{13}CO_2$ adsorption reached equilibrium, the flowing stream was switched to 0.1% $^{12}CO_2$/He without disrupting the CO_2 concentration in the gas phase. These isotopic switch experiments were repeated at different CO_2 concentrations. The Ar inert tracer in one of the mixtures is used to account for hydrodynamic delays and mixing zones that typically corrupt isotopic decay curves. The desorption of $^{13}CO_2$ from the surface and its replacement by $^{12}CO_2$ were measured by on-line mass spectrometry (H200M Gas Analyzer, Leybold-Inficon Inc.) with a time resolution of 2 s. The amount of reversibly adsorbed

S1089-5647(97)02200-1 CCC: $15.00
Published on Web 01/13/1998

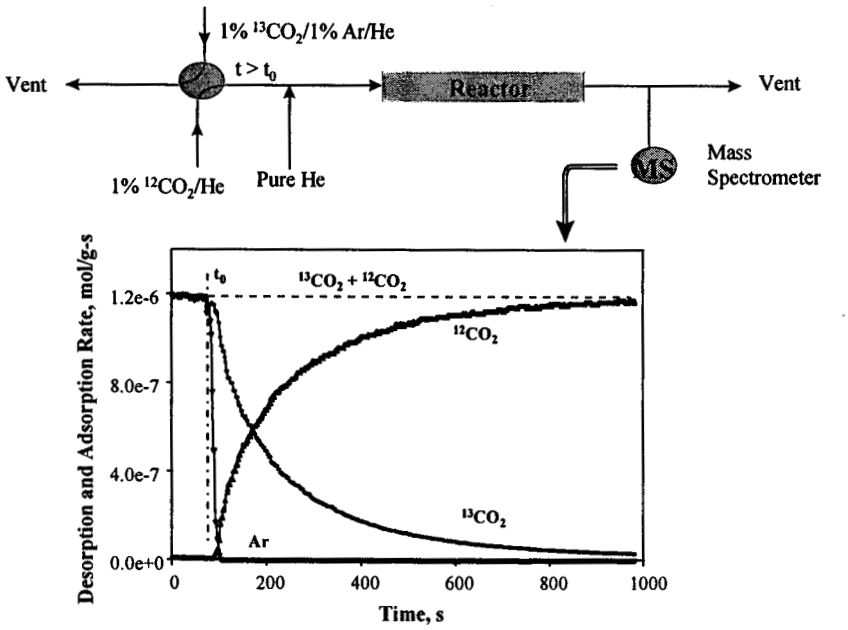

Figure 1. Schematic of steady-state isotopic switch system and isotopic transient obtained on K−$Cu_{0.5}Mg_5CeO_x$ upon switching from $^{13}CO_2$/Ar/He to $^{12}CO_2$/He at 573 K.

$^{13}CO_2$ was calculated from the difference in the areas under the $^{13}CO_2$ and Ar decay curves. Because nonuniform surfaces lead to a distribution of desorption rate constants, desorption rate constants determined from the initial slope of semilogarithmic plots of $^{13}CO_2$ decay data were used to address the effect of CO_2 gas-phase pressure.[14] The initial slope corresponds to the rate constant for first-order desorption from those sites that desorb CO_2 most rapidly at the conditions of our experiments.

Temperature-programmed desorption of $^{13}CO_2$ was carried out by preadsorbing $^{13}CO_2$ at room temperature for 0.16 h on a pretreated sample, flushing with He in order to remove gas-phase and weakly adsorbed $^{13}CO_2$, and increasing the sample temperature to 723 K at 0.5 K/s. $^{13}CO_2$ desorption rates from K−$Cu_{0.5}Mg_5CeO_x$ and K−MgO surfaces in a He stream and in a stream containing various concentrations of $^{12}CO_2$ in He were measured by mass spectrometric analysis of the effluent stream.

Results and Discussion

Figure 1 shows the transient response obtained on a 3.5 wt % K−$Cu_{0.5}Mg_5CeO_x$ catalyst when the isotopic composition of CO_2 was switched at 573 K. As $^{13}CO_2$ was switched to $^{12}CO_2$ at time t_0 without altering the partial pressure or flow rate of CO_2, the concentration of $^{13}CO_2$ decreases as $^{12}CO_2$ concentration increases and the total concentration of CO_2 (i.e., $^{12}CO_2 + ^{13}CO_2$) in the gas phase remains constant. The presence of Ar as an inert tracer permits correction for gas holdup and hydrodynamic delays within the apparatus. The significant delay in the steady-state transient of $^{13}CO_2$, relative to the Ar curve, indicates that the former originates from catalyst-bound $^{13}CO_2$ species that desorb at the temperature of the isotopic exchange experiment within typical catalytic turnover times.

The amount of $^{13}CO_2$ reversibly adsorbed at 573 K, n_e (mol/g), was calculated from the areas under $^{13}CO_2$ and Ar decay curves after correcting mass spectral data for their respective response factors. An isotherm for reversibly adsorbed $^{13}CO_2$ was obtained by relating n_e to C_0, the gas-phase concentration of CO_2 ($^{13}CO_2 + ^{12}CO_2$). The results are shown in Figure 2. The amount of CO_2 adsorbed (n_e) increases slightly from 3.8 $\times 10^{-4}$ to 4.7 $\times 10^{-4}$ mol/g as the CO_2 gas-phase concentration increases by an order of magnitude. This is consistent with a Langmuir-type adsorption isotherm (eq 1) as the surface approaches saturation coverage.

$$n_e = \frac{KC_0}{1 + KC_0} n_s \tag{1}$$

where K is the adsorption equilibrium constant and n_s is the amount of $^{13}CO_2$ reversibly adsorbed at saturation coverage.

The number of $^{13}CO_2$ molecules adsorbed at 573 K and a CO_2 gas-phase concentration of 2.1 $\times 10^{-7}$ mol/cm^3 is 4.7 $\times 10^{-4}$ mol/g, corresponding to a surface density of CO_2-binding sites of 7.6 $\times 10^{-6}$ mol/m^2 on 3.5 wt % K−$Cu_{0.5}Mg_5CeO_x$. The density of surface oxygen atoms on pure MgO is about 18.3 $\times 10^{-6}$ mol/m^2,[21] suggesting that about 40% of the surface oxygen atoms reversibly adsorb $^{13}CO_2$ at 573 K. The actual $^{13}CO_2$ surface coverage may be greater than 0.4 since some of the adsorbed $^{13}CO_2$ desorbs at an undetectable rate at 573 K and the surface of 3.5 wt % K−$Cu_{0.5}Mg_5CeO_x$ contains other components contributing to its surface area.

As discussed previously,[14] CO_2 desorption processes are first-order in surface concentration, and the local slope of a transient decay curve plotted in a semilogarithmic scale gives the desorption rate constant. A large value of this slope reflects rapid desorption and a large value of this rate constant. In Figure 3a, the slope of the transient decay curve at short times, and therefore the desorption rate constant for sites with the highest desorption rates, increases with increasing concentration of CO_2 in the gas phase. As discussed in the Introduction section, the enhancement of desorption rates by gas-phase CO_2 could then be attributed to the higher surface coverage of adsorbed CO_2 present at the higher gas-phase concentration levels. In such a proposal, repulsive interactions among adsorbed CO_2 would then lead to lower desorption activation energies as CO_2 coverages increase and therefore to faster desorption processes. In this study, the surface coverage by reversibly adsorbed CO_2 increases only from 6.1 $\times 10^{-6}$ to 7.6 $\times 10^{-6}$ mol/m^2 as CO_2 gas-phase concentrations increase from 2.1 $\times 10^{-8}$ to 2.1 $\times 10^{-7}$ mol/cm^3. The large change in desorption rate constant appears surprising, in view of the limited

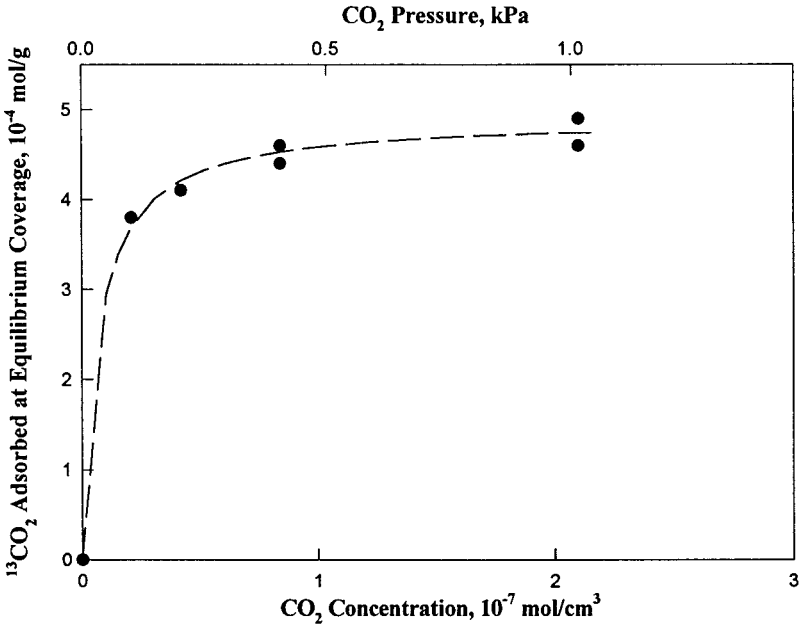

Figure 2. Adsorption isotherm of $^{13}CO_2$ on 3.5 wt % K−$Cu_{0.5}Mg_5CeO_x$ at 573 K (1.7×10^8 cm^3/mol).

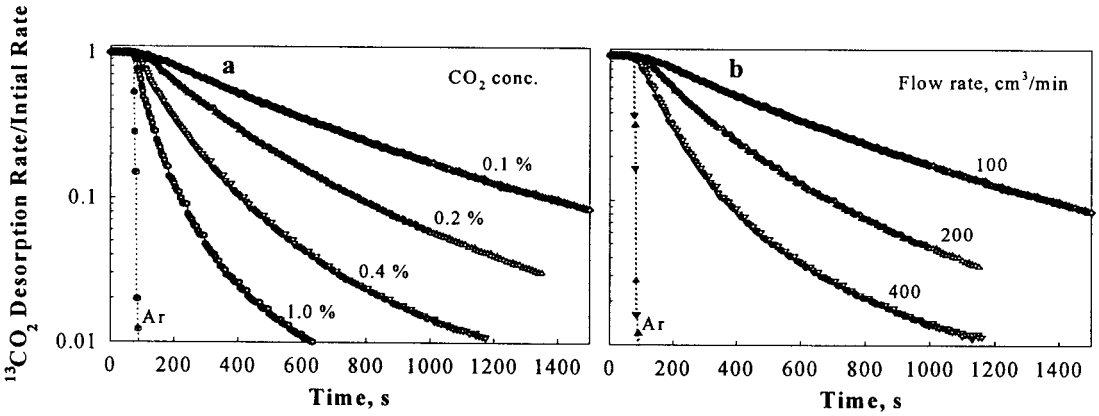

Figure 3. Effects of CO_2 concentration and total flow rate on the desorption rate of preadsorbed CO_2 on a 3.5 wt % K−$Cu_{0.5}Mg_5CeO_x$ catalyst [75 mg catalyst charge, 573 K].

range of surface densities giving rise to these marked changes in kinetic parameters.

In our experiments, the desorption rate constant for adsorbed $^{13}CO_2$, however, depends not only on the concentration of $^{12}CO_2$ in the gas phase but also on the flow rate of the carrier stream carrying this $^{12}CO_2$ (Figure 3b). Desorption rate constants appear to increase with increasing carrier gas flow rate. Clearly, changes in surface coverage alone cannot account for these effects, because in the absence of readsorption the surface coverage cannot be influenced by the rate at which desorption products are removed by a carrier gas. The surface is always in chemical equilibrium with the gas phase, and this equilibrium surface coverage is controlled only by the temperature and the CO_2 concentration in the gas-phase, neither of which changes with changes in carrier gas flow rate. Thus, changes in desorption activation energies caused by differences in surface coverage cannot account for the effects of flow rate on the apparent desorption rate constant (Figure 3b). We consider below the proposal that readsorption of desorbed CO_2 accounts for both gas-phase concentration and flow rate effects on the rate of $^{13}CO_2$ desorption.

The promoting effect of the gas phase on desorption rates was previously reported for desorption of CO from group VIII transition metals. Our study shows that such effects appear to be quite general and apply to a different adsorbate on metal oxide surfaces. In a previous study, Herz et al.[22] carried out temperature-programmed desorption studies of CO on a thin wafer of a supported Pt catalyst and showed that significant readsorption occurred whether the desorption of CO took place in a flowing carrier gas or in a high-vacuum system. In fact, adsorption−desorption equilibrium was approached closely during desorption and the obtained desorption spectra reflected the thermodynamics, rather than the kinetics of desorption. The conditions of these experiments by Herz et al.[22] were typical of most experimental studies of CO desorption from catalytic solids. The increase in $^{13}CO_2$ desorption rate with increasing $^{12}CO_2$ gas-phase concentration or increasing carrier flow rate can be explained by taking into account the ubiquitous readsorption of the desorbed $^{13}CO_2$ during our experiments. Readsorption effects may also be able to account for the similar effects previously attributed to "adsorption-assisted" phenomena.[2,3]

For a given sample, the number of adsorption sites, n_s (mol/g), occupied by CO_2 when all surface sites are covered (*saturation coverage*) is independent of flow rate and gas-phase composition. At conditions of chemical equilibrium, the number of adsorption sites, n_e, actually occupied by CO_2 increases with gas-phase CO_2 concentration, initially in a linear manner but

then only slightly as saturation coverages are approached (eq 1). The number of unoccupied adsorption sites (n_s-n_e) at equilibrium is small and inversely proportional to the CO_2 gas-phase concentration at conditions approaching saturation coverage, as shown by eq 2 as the KC_o term in the denominator becomes larger than unity:

$$n_s - n_e = \frac{n_s}{1 + KC_0} \tag{2}$$

Therefore, the density of unoccupied adsorption sites ($n_s - n_e$) decreases and the probability that desorbed $^{13}CO_2$ will readsorb also decreases with increasing concentration of $^{12}CO_2$ in the gas phase. In effect, as CO_2 gas-phase concentration or carrier gas flow rate increase, we measure a net desorption rate that becomes closer to the intrinsic (unidirectional) rate of desorption, uncorrupted by its reverse step, the readsorption of $^{13}CO_2$. It should be pointed out that we only treat the initial part of the decay, that is, the compartment on the surface with the fastest desorption rate, using a Langmuir-type adsorption isotherm.

A rigorous mole balance on $^{13}CO_2$ in a flow system subjected to a $^{13}CO_2$ to $^{12}CO_2$ switch at zero time is given by

$$-\left[\left(\frac{d}{dt}\theta^{13}\right)N_s\right] = k_d\theta^{13}N_s - k_aC^{13}(N_s - N_e) \tag{3}$$

and

$$-\left[\left(\frac{d}{dt}\theta^{13}\right)N_s\right] = FC^{13} \tag{4}$$

when the pseudo-steady-state hypothesis is valid. In this hypothesis, $^{13}CO_2$ desorption rate from the surface equals the rate of $^{13}CO_2$ coming out of the reactor. This is valid only when the void volume of the catalyst bed is small and therefore no accumulation of $^{13}CO_2$ in the void volume shortly after CO_2 isotopic switch. In these expressions, θ^{13} is the fraction of adsorption sites occupied by $^{13}CO_2$ at any time after the switch, C^{13} is the gas-phase concentration of $^{13}CO_2$ (mol/cm^3), C_0 is the total gas-phase concentration of CO_2, irrespective of isotopic label (mol/cm^3), N_s is the number of adsorption sites occupied by CO_2 at *saturation* coverage (mol), N_e is the number of adsorption sites occupied by CO_2 at thermodynamic equilibrium (mol), F is the volumetric gas flow rate (cm^3/s), and k_a (cm^3/(mol s)) and k_d (s^{-1}) are the adsorption and desorption rate constants, respectively. The solution to the above equations describes the decay curve for $^{13}CO_2$ concentration in the effluent:

$$C^{13} = \frac{N_ek_d}{F + \frac{N_ek_d}{C_0}} \exp\left[-\frac{k_d}{1 + \frac{N_ek_d}{FC_0}}t\right] \tag{5}$$

We note that if we define an apparent desorption rate constant k_d':

$$k'_d = \frac{k_d}{1 + \frac{N_ek_d}{FC_0}} \tag{6}$$

Equation 5 can then be rewritten as:

$$r^{13} = FC^{13} = N_ek'_d \exp(-k'_dt) \tag{7}$$

The desorption rate corresponds to that for a first-order rate expression with a pseudokinetic rate constant k_d', which can be obtained from the initial slope of a semilogarithmic plot. As shown by eq 6, this apparent rate constant carries kinetic information (k_d), but also experimental variables, such as carrier gas flow rate and CO_2 gas-phase concentration, and thermodynamic properties reflected in the value of N_e. Measurements of the unidirectional rate of desorption using initial slopes are corrupted by the presence of a significant rate of the reverse reaction—the readsorption of desorbed $^{13}CO_2$—as desorbed molecules exit the sample cell.

The apparent rate constant defined by eq 6 can be rewritten as

$$\frac{1}{k'_d} = \frac{1}{k_d} + \frac{W_gn_e}{C_0}\frac{1}{F} \tag{8}$$

where W_g is the mass of sample used (g) and n_e (N_e/W_g) is the density of sites available for CO_2 adsorption−desorption processes (mol/(g-cat)) at a given temperature on a given sample. This site density is unaffected by readsorption processes and independent of carrier gas flow rate; it is obtained directly from the area under the $^{13}CO_2$ decay curves. A description of the dynamics of these decay curves, however, requires that we account for readsorption effects that decrease the net rate of desorption of $^{13}CO_2$ from surfaces.

For a given material and mass of sample, we observe that the apparent rate constant k_d' increases with increasing flow rate and gas-phase CO_2 concentration (Figure 3a,b). The reciprocal of the value of k_d' (obtained from the initial slope of the semilogarithmic plot of the data in Figure 3) is plotted as a function of the reciprocals of CO_2 concentration and flow rate in Figure 4a,b, respectively. The linear plots in Figure 4a,b are consistent with the form of the apparent desorption rate constant suggested by eq 8. The slopes in Figure 4 depend only on the equilibrium amount of adsorbed CO_2 (n_e) at 573 K. It should be pointed out that n_e does not change with increasing carrier flow rate, but increases slightly as CO_2 gas-phase concentration increases from 2.1×10^{-8} to 2.1×10^{-7} mol/cm^3. The increase in the apparent desorption rate constant of $^{13}CO_2$ with increasing carrier gas flow rate and gas-phase CO_2 concentration has also been observed on 1.0 wt % K−MgO samples. It should be noticed that $1/k_d'$ approaches zero as the value of the abscissa decreases, suggesting that the intrinsic rate of desorption is very large. These values reflect the dynamic behavior of those sites that desorb CO_2 at the fastest rate that can be measured given our hydrodynamic delays. Thus, it is not surprising that the unidirectional rate constant for such sites is too fast to be accurately detected by our experiments.

These data show that higher $^{12}CO_2$ gas-phase concentrations lead to higher net $^{13}CO_2$ desorption rates because the probability that a desorbed $^{13}CO_2$ molecule will readsorb decreases with increasing surface coverage of CO_2 species, irrespective of their isotopic label, and with decreasing density of unoccupied adsorption sites. The desorption rate constant reported by Tamaru et al.[3] for CO on Pd polycrystalline surfaces may have also been influenced by readsorption phenomena because the rate of desorption was measured under such conditions that adsorption was also taking place. If unlabeled gas-phase CO can adsorb on Pd polycrystalline surfaces during the desorption process of labeled CO, it is reasonable to expect the occurrence of readsorption of the desorbed CO and the relative rates depend exclusively on the abundance of the two isotopes in the gas phase. As reported by Tamaru et al.,[3] the surface concentration

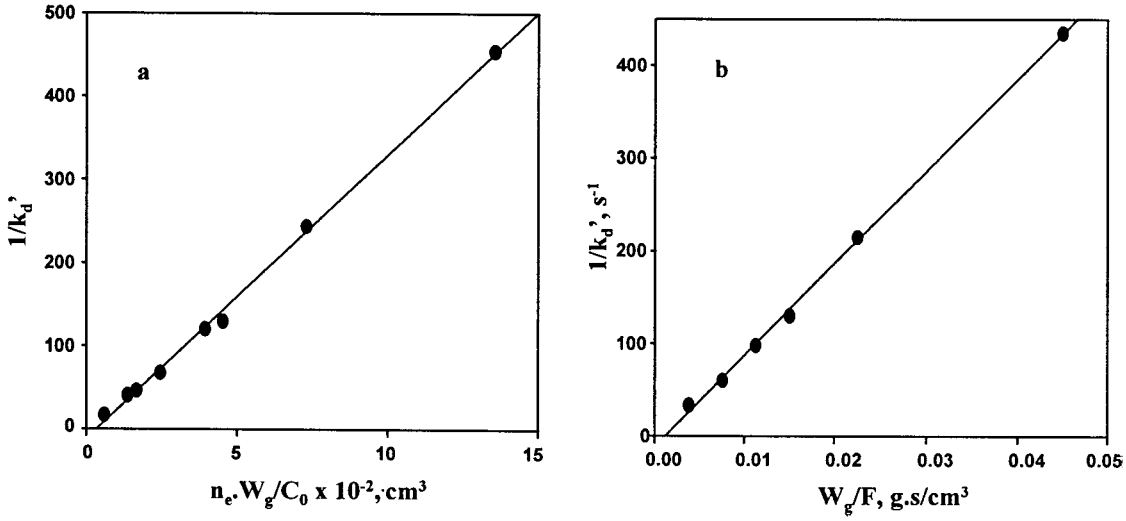

Figure 4. Effects of total gas-phase CO_2 concentration (C_0), carrier gas flow rate (F), and amount of sample on the apparent desorption rate constant (k_d') for $^{13}CO_2$ desorption from 3.5 wt % K−$Cu_{0.5}Mg_5CeO_x$ at 573 K.

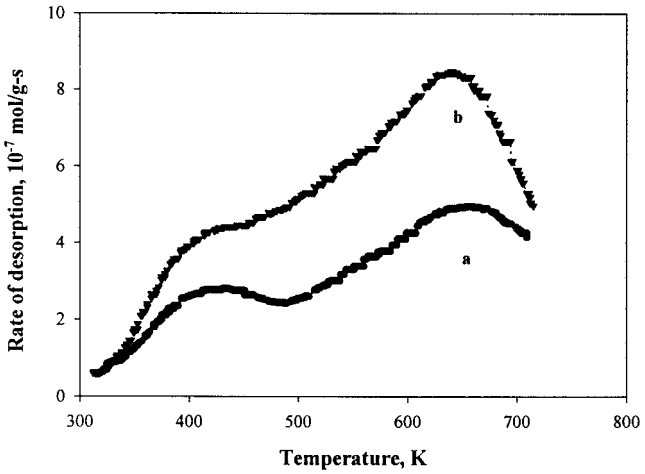

Figure 5. $^{13}CO_2$ TPD from 3.5 wt % K−$Cu_{0.5}Mg_5CeO_x$ (a) in He and (b) in 0.1% $^{12}CO_2$/He [25 mg catalyst charge, 200 cm^3/min].

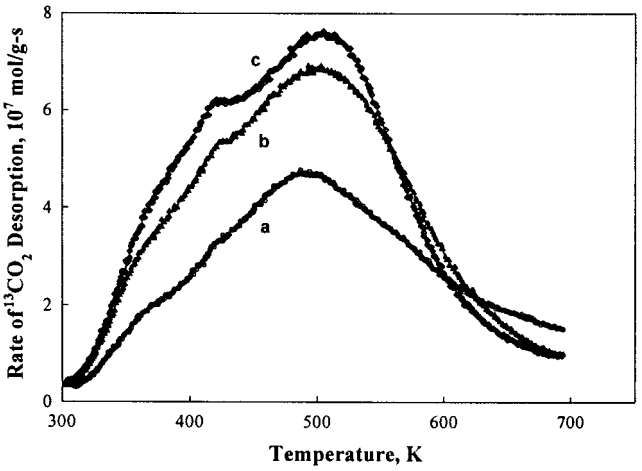

Figure 6. $^{13}CO_2$ TPD from 1.0 wt % K−MgO (a) in He, (b) in 0.1% $^{12}CO_2$/He, and (c) in 0.4% $^{12}CO_2$/He [25 mg catalyst charge, 200 cm^3/min].

of CO increases by less than 5% as the gas-phase CO pressure increased from 2×10^{-6} to 13×10^{-6} Pa at 339 K, suggesting that the surface is almost saturated with adsorbed CO. Although the surface CO concentration increases slightly, the desorption rate constant increases by at least a factor of 2. It is surprising that the enhanced intermolecular repulsive interaction due to the slightly increased surface coverage could cause the dramatic increase in CO_2 desorption rate. The kinetic parameter that characterizes the unidirectional desorption rate may be much larger than those measured when readsorption occurs during desorption processes. At higher CO_2 pressure, fewer vacant sites are available for readsorption of the desorbed $^{13}CO_2$ and desorption rates approach their values for the unidirectional desorption process.

Significant readsorption of desorbed $^{13}CO_2$ occurs during isotopic switch experiments with 0.1% $^{12}CO_2$/He as a carrier on K-promoted $Cu_{0.5}Mg_5CeO_x$ even at the highest carrier flow rates (200 cm^3/min) and smallest catalyst samples (25 mg). The corresponding residence times within the sample bed at these conditions are expected to be shorter than those used in typical temperature-programmed desorption studies of CO_2 on basic oxides (typical flow rate is 200 cm^3/min for 50−100 mg of catalyst).[23]

Figure 5 shows the temperature-programmed desorption spectrum of $^{13}CO_2$ preadsorbed on 3.5 wt % K−$Cu_{0.5}Mg_5CeO_x$ (25 mg) when the carrier gas is pure He (200 cm^3/min) (curve a). Two distinct peaks with different intensity appear at about 434 and 656 K. When 0.1% $^{12}CO_2$/He is used as the carrier gas, the $^{13}CO_2$ TPD spectrum shifts to lower desorption temperatures, but retains the two peaks with intensities higher than those observed in a He carrier gas (Figure 5, curve b). The high-temperature desorption peak decreases from 656 to 640 K and the low-temperature feature appears to move to even lower temperature when gas-phase $^{12}CO_2$ is present. The number of desorbed $^{13}CO_2$ molecules is significantly larger when $^{12}CO_2$ is present in the carrier gas stream. If the desorption temperature kept increasing, the total number of desorbed $^{13}CO_2$ molecules in He and 0.1% $^{12}CO_2$/He streams would reach the same value, because the number of preadsorbed $^{13}CO_2$ is identical in these two experiments.

The promoting effect of gas-phase $^{12}CO_2$ on the observed $^{13}CO_2$ desorption rate has also been observed on 1.0 wt % K−MgO, as evidenced by the increased desorption rate in the presence of 0.1% $^{12}CO_2$ (Figure 6). Increasing $^{12}CO_2$ concentration results in further increase in the desorption rate. It should be pointed out that the presence of gas-phase $^{12}CO_2$ causes the disappearance of the shoulder peak around 570−580 K observed in He flow (Figure 6, curve a). The presence of gas-phase $^{12}CO_2$ may shift this peak to lower temperatures because readsorption

is inhibited when $^{12}CO_2$ adsorbs on otherwise unoccupied surface sites. Since there are at least four desorption peaks (around 370, 425, 500, and 580 K) in the $^{13}CO_2$ TPD spectrum in He flow (Figure 6, curve a), it is difficult to establish which peak in curves b and c corresponds to the peak in curve a. The minimization of readsorption in the presence of gas-phase CO_2 shifts desorption peaks to significantly lower temperatures.

The surface coverage of $^{13}CO_2$ for a given sample at the start of the temperature ramp is identical in these types of TPD experiments. In the presence of $^{12}CO_2$, however, the total surface coverage of CO_2 ($^{13}CO_2 + {}^{12}CO_2$) is higher at every temperature than when pure He is used as the carrier gas. Meanwhile, the probability of readsorption increases as $^{13}CO_2$ desorbs from the surface and unoccupied adsorption sites rapidly form, until at higher temperatures the surface is almost bare and the sticking coefficient for colliding CO_2 molecules is very high. In the presence of a constant gas-phase concentration of $^{12}CO_2$, the total surface coverage of CO_2 remains higher at every temperature and depends only on the equilibrium coverage at each temperature. Then, as $^{13}CO_2$ is depleted from the surface, vacant adsorption sites are occupied by the majority $^{12}CO_2$ species in the gas phase; therefore, readsorption of desorbed $^{13}CO_2$ is minimized. It is well-known that readsorption will shift desorption peaks to higher temperatures.[22] Thus, it is not surprising that higher gas-phase $^{12}CO_2$ concentrations, which minimize readsorption, lead to a shift of desorption peaks to lower temperatures. The higher temperature $^{13}CO_2$ desorption peak, or at least the part of it detected with He as a carrier gas (Figures 5 and 6), reflects the desorption of $^{13}CO_2$ molecules that readsorbed after their initial desorption at lower temperatures.

Conclusions

CO_2 desorption rates from basic oxide surfaces, such as those found in K−MgO and K−$Cu_{0.5}Mg_5CeO_x$, increase as the gas-phase CO_2 concentration and carrier gas flow rate increase. These effects resemble those attributed previously to adsorption-assisted desorption phenomena, but our isotopic switch studies and a detailed analysis of the kinetics of reversible adsorption−desorption processes on surfaces show that they reflect instead the expected inhibition of readsorption steps at higher surface coverages or shorter bed residence times. Intermolecular interactions between adsorbed CO_2 molecules or kinetic assistance of desorption by concurrent adsorption steps are not required to explain these phenomena on modified MgO. Actually, such explanations would not account for any effects of gas flow rate on the net rate of desorption.

We cannot, however, rule out a role of adsorption-assisted desorption of CO on metal surfaces, for which such kinetic phenomena were first proposed. Unidirectional desorption rates can become corrupted by readsorption events during temperature-programmed desorption of preadsorbed CO_2 on these metal oxides. Isotopic switch methods or temperature-programmed desorption of preadsorbed $^{13}CO_2$ into a gas stream containing $^{12}CO_2$ probe more directly the kinetics of the unidirectional desorption processes on real catalytic solids at conditions typical of catalytic reactions. Our study shows that the mechanism of desorption at chemical and isotopic equilibrium remains valid as changes in gas-phase concentration perturb the position of this equilibrium. In contrast, adsorption-assisted desorption requires that elementary desorption steps proceed via elementary steps that depend on the composition of the contacting gas phase.

Acknowledgment. The authors acknowledge the assistance of Dr. Marcelo Gines in the synthesis and characterization of the modified MgO samples and Professor Michel Boudart (Stanford University) for helpful technical discussions on the subject of this article.

References and Notes

(1) Yamada, T.; Tamaru, K. *Surf. Sci.* **1984**, *146*, 341.
(2) Yamada, T.; Tamaru, K. *Surf. Sci.* **1984**, *138*, L155.
(3) Yamada, T.; Onishi, T.; Tamaru, K. *Surf. Sci.* **1983**, *133*, 533.
(4) Tamaru, K. *Bull. Chem. Soc. Jpn.* **1996**, *69*, 961.
(5) Takagi, N.; Yoshinobu, J.; Kawai, M. *Chem. Phys. Lett.* **1993**, *215*, 120.
(6) Yates, J. T., Jr.; Goodman, D. W. *J. Chem. Phys.* **1980**, *73* (10), 5371.
(7) Yamada, T.; Zhai, R.; Iwasawa, Y.; Tamaru, K. *Bull. Chem. Soc. Jpn.* **1987**, *62*, 2387.
(8) Parker, D. H.; Fischer, D. A.; Colbert, J.; Koel, B. E.; Gland, J. L. *Surf. Sci.* **1991**, *258*, 75.
(9) Schroder, U.; Schnoon, N.-H. *J. Catal*. **1993**, *43*, 369.
(10) Zhdanov, V. P. *Surf. Sci.* **1985**, *157*, L384.
(11) Lombardo, S. J.; Bell, A. T. *Surf. Sci*. **1991**, *245*, 213.
(12) Lauterbach, J.; Sushchikh, M.; Weinberg, W. H. *Z. Phys. Chem.* **1997**, *198*, 99.
(13) Xu, M.; Gines, M. J. L.; Hilmen, A.-M.; Stephens, B. L.; Iglesia, E. *J. Catal.* **1997**, *171*, 130.
(14) Xu, M.; Iglesia, E. To be submitted to *J. Phys. Chem.*
(15) Tamaru, K. *Dynamic Heterogeneous Catalysis*; New York, 1978.
(16) Happel, J.; Cheh, H. Y.; Otarod, M.; Ozawa, S.; Severdia, A. J.; Yoshida, T.; Fthenakis, V. *J. Catal*. **1982**, *75*, 314.
(17) Otarod, M.; Ozawa, S.; Yin, F.; Chew, M.; Cheh, H. Y.; Happel, J. *J. Catal*. **1983**, *84*, 156.
(18) Biloen, P.; Helle, J. N.; van der Berg, F. G. A.; Sachtler, W. H. M. *J. Catal*. **1983**, *80*, 450.
(19) DePontes, M.; Yokomizo, G. H.; Bell, A. T. *J. Catal*. **1987**, *104*, 147.
(20) Shannon, S. L.; Goodwin, J. G. *Chem. Rev.* **1995**, *95*, 677.
(21) McKenzie, A. L.; Fishel, C. T.; Davis, R. J. *J. Catal*. **1992**, *138*, 547.
(22) Herz, R. K.; Kiela, J. B.; Marin, S. P. *J. Catal*. **1982**, *73*, 66.
(23) Falconer, J. L.; Schwarz, J. A. *Catal. Rev.-Sci. Eng*. **1983**, *25* (2), 141.